Electromagnetic Transient (EMT) Simulation Algorithm for Evaluation of Photovoltaic (PV) Generation Systems

Jongchan Choi
Power Electronics Systems Integration
Oak Ridge National Laboratory
Oak Ridge, USA
choij1@ornl.gov

Suman Debnath
Power Electronics Systems Integration
Oak Ridge National Laboratory
Oak Ridge, USA
debnaths@ornl.gov

***Abstract*—Use of inverter-based resources facilitating renewable energy resources such as photovoltaic (PV) generation is increasing rapidly with decreasing costs and reduced emissions associated. To accommodate such rapid growth of inverter-based resources like PV systems, electromagnetic transient (EMT) simulation models of both PV systems and grids are required to analyze the interaction of PVs in the grid (like the post-event analysis). In addition, the EMT simulation would help with the planning of future power grid with a large number of PVs as well as other inverter-based distributed generation systems. In this paper, the EMT simulation models of PV systems and grids are developed based on the differential algebraic equations (DAEs) representing their EMT dynamics. Furthermore, advanced simulation algorithms including numerical stiffness-based hybrid discretization, DAE clustering and aggregation, multi-order integration, and matrix splitting approaches are applied to accelerate the EMT simulation. The proposed algorithm was applied to 125 PV inverters within 52-bus medium-voltage (MV) distribution grid.**

Keywords—Electromagnetic transient, Distribution grids, Distributed generation, Photovoltaic, inverter-based resources

I. INTRODUCTION

Inverter-based generation systems such as photovoltaic (PV) systems, wind power plant, and energy storage systems are rapidly deploying due to reduced costs and environmental benefits associated. The U.S. Energy Information Administration (EIA) forecasts that the share of renewable energy in U.S. electricity generation will increase up to 42% by 2050 [1]. In addition, EIA highlights that wind and solar generation will be responsible for most of the share in the growth. Higher growth than the aforementioned estimate may happen based on policy changes. Such growth will rapidly increase the penetration of inverter-based resources in a grid.

With the high penetration of inverter-based resources in grids, EMT simulation is necessary to analyze the interaction of inverters with the rest of the system in the grid. The analysis may include studies to understand control interaction, instability, impact of unbalanced fault, post fault analysis, etc. Many reports have pointed out the fact that such EMT simulation requirement is critical to analyze accurate dynamics of inverters and grids. Reliability guideline from NERC recommends using EMT modeling to study certain reliability issues when inverters-based resources are connected in short electrical distance, in low short-circuit strength grid, in proximity to series capacitor among others [2]. Some challenges have been reported that inverter control instability may not be detectable without EMT simulation model because the instability was introduced by fast inner loop controllers in inverters [3]. Other issues that requirement an EMT simulation model include the recent events of unbalanced fault in California that resulted in a disconnection of large-scale PV power plants and distributed energy resources from the power grid [4]–[6]. To analyze the impact of such events on inverter-based resources, high-fidelity switching models of the inverters and EMT models of power grids are required. However, simulations of these high-fidelity EMT models can get time consuming and impose heavy computational burden.

To overcome the computational challenges in EMT simulations, there have been several researches conducted in the past. Some of the researches applied numerical stiffness-based hybrid discretization method to power electronics components and small electrical power grid studies in EMT simulations. Based on the stiffness properties, hybrid backward Euler and forward Euler discretization was applied in the studies to speed up EMT simulation [7]–[9]. Kron's reduction for linear system equations and its variants have also been applied to electrical power grid networks for simulation speed up and node reductions [10]–[13].

In this paper, differential algebraic equations (DAEs) clustering and aggregation, multi-order integration approach,

Research sponsored by Solar Energy Technologies Office of U.S. Department of Energy. This material is based upon work supported by the U.S. Department of Energy's Office of Energy Efficiency and Renewable Energy (EERE) under the Solar Energy Technologies Office Award Number 36532. The views expressed herein do not necessarily represent the views of the U.S. Department of Energy or the United States Government.

Jongchan Choi and Suman Debnath are with Oak Ridge National Laboratory, Knoxville, TN 37932, USA (email: choij1@ornl.gov).

and, matrix splitting along with numerical stiffness-based hybrid discretization has been applied to EMT simulation models. The models include that of a dc-dc boost converter, a dc-ac inverter, LCL filter, distribution transformer, and distribution feeder lines, to represent and evaluate EMT dynamics of large PV plant of multiple distributed PV in a grid.

II. System Description and EMT Modeling

The system configuration of a PV inverter module, a distribution transformer collecting multiple PV inverter modules, and a distribution grid including multiple distribution transformers is described. In addition, the EMT models associated with the individual components and the systems are derived based on states to form differential algebraic equations (DAEs) in this section.

A. PV Distributed Generation System

The PV inverter module considered in this paper consists of a 5-point PV array representing PV characteristics, a dc-dc boost converter, an ac-dc three-phase voltage source inverter, and a LCL filter. The PV inverter module is illustrated in Fig. 1.

The EMT model of the PV inverter module can be expressed by the DAEs provided below:

$$C_{\text{pv}}\frac{dv_{c,\text{pv}}}{dt} = -\left(\frac{v_{c,\text{pv}}}{R_{C,\text{dc}}}\right) - i_{L_{\text{pv}}} + i_{\text{pv}} \tag{1}$$

$$L_{\text{pv}}\frac{di_{L_{\text{pv}}}}{dt} = -R_{L,\text{dc}}i_{L_{\text{pv}}} + v_{c,\text{pv}} - v_{\text{dc}}\left\{S_{2,\text{dc}}(1-S_{1,\text{dc}}) + (1-S_{2,\text{dc}})(1-S_{1,\text{dc}})\,\text{sgn}\left(i_{L_{\text{pv}}}\right)\right\} \tag{2}$$

$$C_{dc}\frac{dv_{dc}}{dt} = -\frac{v_{dc}}{R_{dc}} + i_{L,pv}\{S_{2,dc}(1-S_{1,dc}) + (1-S_{2,dc})(1-S_{1,dc})\,\text{sgn}(i_{L,pv})\} - i_{j,ac}\{S_{1,j,ac}(1-S_{2,j,ac}) + (1-S_{2,j,ac})(1-S_{1,j,ac})\,\text{sgn}(-i_{j,ac})\} \tag{3}$$

$$L_{1,ac}\frac{di_{j,ac}}{dt} = -R_{1,ac}i_{j,ac} + \frac{v_{dc}}{2}\{S_{1,j,ac}(1-S_{2,j,ac}) - S_{2,j,ac}(1-S_{1,j,ac}) - (1-S_{2,j,ac})(1-S_{1,j,ac})(2\,\text{sgn}(i_{j,ac}) - 1)\} - v_{i.ac.fil} \tag{4}$$

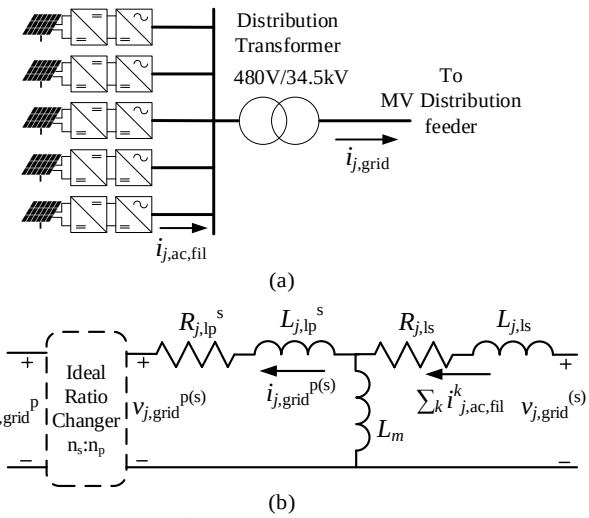

Fig. 2: Distribution transformer with multiple PV inverter modules: (a) configuration of a single distribution transformer collecting five PV inverter modules, (b) transformer model by classical approach.

$$C_{\text{ac}}\frac{dv_{j,\text{ac,fil}}}{dt} = -\frac{v_{j,\text{ac,fil}}}{R_{c,\text{ac}}} + i_{j,\text{ac}} - i_{j,\text{ac,fil}} \tag{5}$$

$$L_{2,\text{ac}}\frac{di_{j,\text{ac,fil}}}{dt} = -R_{2,\text{ac}}i_{j,\text{ac,fil}} + v_{j,\text{ac,fil}} - v^{s}_{j,\text{grid}} \tag{6}$$

B. Multiple PV Inverter Modules Connected through a Single Distribution Transformer

Multiple PV inverter modules can be connected to a single distribution transformer between the medium voltage (34.5kV) and low-voltage (480V) distribution grids. The number of the connected PV inverter modules can be up to five in this paper. The single distribution transformer with multiple PV inverter modules is illustrated in Fig. 2-(a).

The EMT model of the multiple PV inverter modules in Fig. 2 is modeled by using the DAEs provided below:

$$v^{p(s)}_{j,\text{grid}} = \frac{n_s}{n_p}v^{p}_{j,\text{grid}} \tag{7}$$

$$L_{1s}\frac{d\sum_k i^k_{j,\text{ac,fil}}}{dt} + L^{(s)}_{1p}\frac{di^{P(s)}_{j,\text{grid}}}{dt} = -R_{1s}\sum_k i^k_{j,\text{ac,fil}} - R^{(s)}_{1p}i^{p(s)}_{j,\text{grid}} + v^{(s)}_{j,\text{grid}} - \frac{n_s}{n_p}v^{p}_{j,\text{grid}} \tag{8}$$

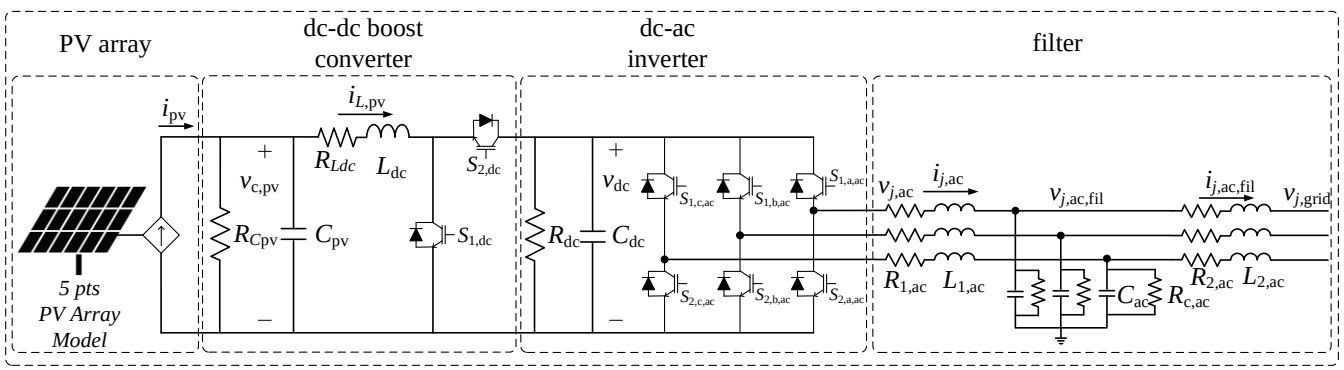

Fig. 1. PV inverter module consisting of PV array, dc-dc converter, dc-ac inverter, LCL filter.

$$L_m^s \frac{d\sum_k i_{j,\text{ac,fil}}^k}{dt} + \left(L_{1p}^s + L_m^s\right) \frac{di_{j,\text{grid}}^{P(s)}}{dt} = R_{1p}^{(s)} i_{j,\text{grid}}^{p(s)} + \frac{n_s}{n_p} v_{j,\text{grid}}^p \quad (9)$$

C. Medium Voltage (MV) Distriution Grid with Multiple Distribution Transformers including Multiple PV Inverter Modules

Large number of PV inverter modules can be deployed widely in a MV distribution grid with distribution lines and distribution transformers. The overall layout of the MV distribution grid with PV inverter modules is illustrated in Fig. 3. The MV distribution grid considered in this paper includes up to 25 distribution transformers containing a total of 125 PV inverter modules. This system may represent a large solar farm as well as a distribution grid with a great number of inverter-based distributed generation systems.

The MV distribution feeder is modeled by three phase PI section model to represent mutual coupling effects between the lines. The three phase PI section model between node n and m is illustrated in Fig. 4. The EMT model of the PI section line in Fig. 4 is described by using the DAEs provided below (phase A only):

$$L_{aa} \frac{di_{a,line}}{dt} + R_{aa} i_{a,line} + L_{ab} \frac{di_{a,line}}{dt} + R_{ab} i_{a,line} + L_{ac} \frac{di_{a,line}}{dt} + R_{ac} i_{a,line} = v_{a,n} - v_{a,m} \quad (10)$$

$$C_{aa} \frac{dv_{a,n}}{dt} + C_{ab} \frac{dv_{a,n}}{dt} + C_{ac} \frac{dv_{a,n}}{dt} = i_{a,n} - i_{a,line} \quad (11)$$

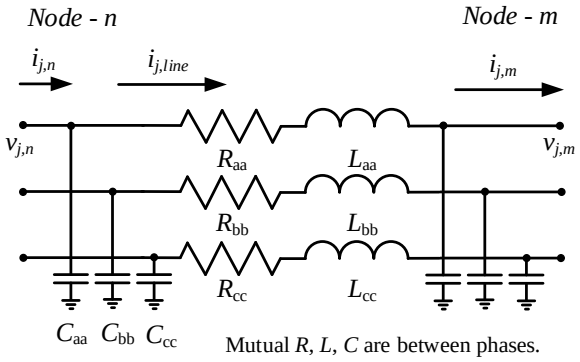

Fig. 4: Three phase PI section line model for distribution main and lateral feeders.

The distribution feeder lines considered in this paper are of two types: main feeder line and lateral feeder line as shown in Fig. 3. The line lengths of main feeder and lateral feeder are considered as 60 meters and 30 meters in this paper, respectively.

III. Advanced EMT Simulation Algorithm for Simulation Speed Acceleration

Advanced simulation algorithms including DAEs' numerical stiffness-based hybrid discretization, DAEs clustering and aggregation, multi-order integration, and matrix splitting method are applied on the individual components and the systems described in Section II to accelerate the speed of EMT simulation.

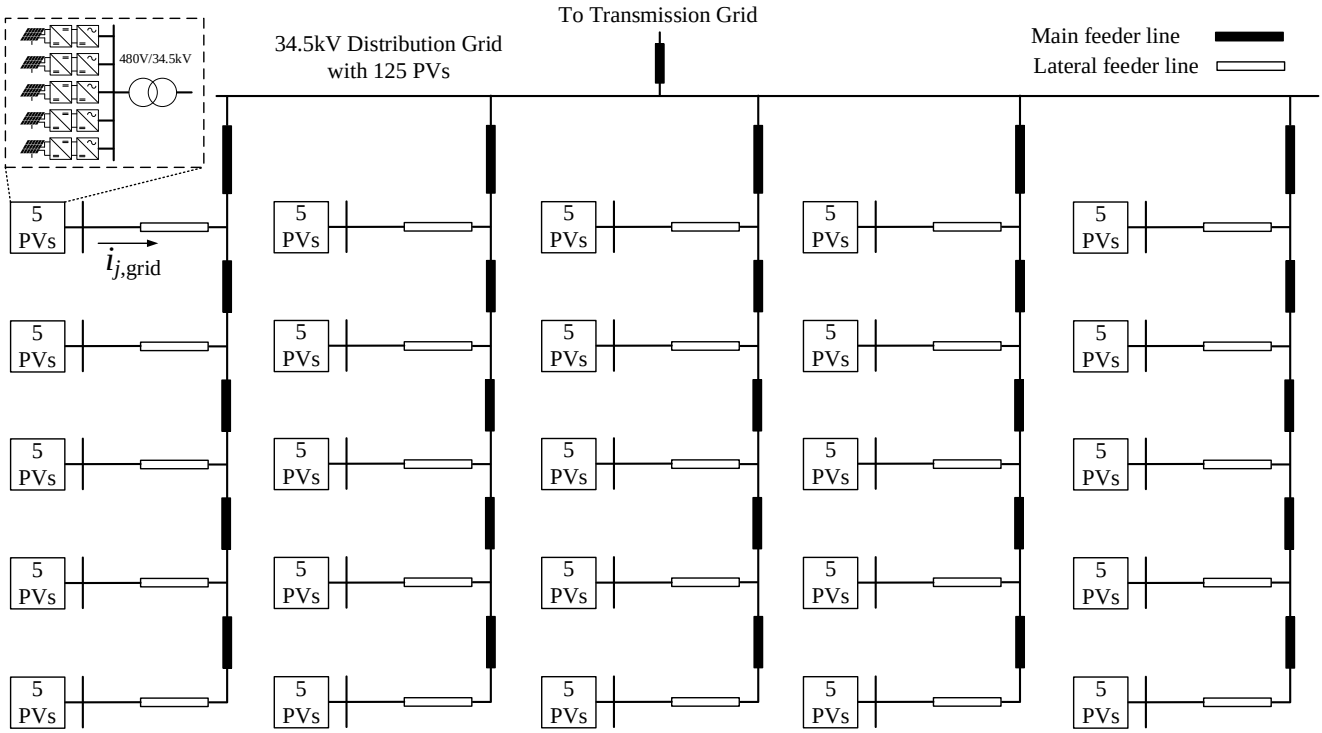

Fig. 3: 52-bus medium voltage (MV) distribution grid with 25 distribution transformers and 125 PV inverter modules.

The DAEs representing the dynamics of the individual PV inverter module in Fig. 1 can be segregated based on numerical stiffness property of DAEs [5]. In the PV inverter module, the DAEs representing the dynamics of the inductor current of the dc-dc converter ($i_{L,\mathrm{pv}}$), the dc-ac inverter current ($i_{j,\mathrm{ac}}$), the filter voltage ($v_{j,\mathrm{ac,fil}}$), and the filter current ($i_{j,\mathrm{ac,fil}}$) present numerical stiffness characteristic. The DAEs with the numerical stiffness are discretized by backward Euler method. On the other hand, the DAEs representing the dynamics of capacitor voltages of the dc-dc boost converter ($v_{\mathrm{c,pv}}$ and v_{dc}) have numerical non-stiffness characteristic. The DAEs with non-stiffness are discretized by forward Euler method. By this segregation based on the numerical stiffness, simulation time taken for the EMT model is greatly reduced while maintaining high accuracy and stability.

The DAEs representing the dynamics of the multiple PV inverter modules with the single transformer in Fig. 2 can be aggregated by clustering the similar dynamics across the multiple PV inverter modules. By grouping the DAEs, a large matrix required to be inverted in computation can be reduced into a smaller one. This method mitigates the computational burden of the large matrix inversion to speed up the EMT simulation.

A multi-order integration approach such as the trapezoidal integration method is applied to the DAEs representing the dynamics of distribution feeders and lines to enable use of higher simulation timestep in the simulation as compared to smaller one for switching dynamics in the PV inverter module. With the multi-order discretization, the DAEs representing the MV distribution grid can be formed in large linear system equations, Ax=b. The size of the A matrix is essentially dependent on the number of nodes in the MV distribution grid, and the large A matrix increases to run simulations.

EMT simulation time for a large distribution grid increases as the number of nodes in the grid increases. Since the size of A matrix can create a bottleneck in the computation, a matrix splitting method is applied to decrease the size of A matrix by dividing the MV distribution grid into multiple subsystems that have similar dynamics. For example, the MV distribution grid in Fig. 3 can be divided into six subsystems consisting of five radial feeders and a collector bus. When dividing the MV grid into subsystems to split the A matrix, a single time step delay is introduced in the transferred states between the subsystems. To prevent numerical instability from the single delayed states, small capacitors are added to the terminal nodes of each subsystems to reduce a rapid change in the delayed states.

An overview of the application of these algorithms is shown in Fig. 5.

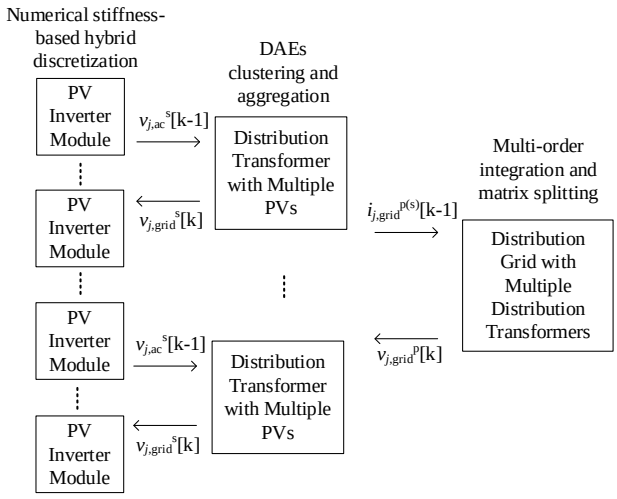

Fig. 5: Overview of the advanced simulation algorithm for the large number of PV systems in MV distribution grid.

IV. Simulation Results

The grid with PV inverter modules in Fig. 3 is simulated using two different approaches: single A matrix and multiple A matrices for the MV distribution grid with 52 nodes, 25 distribution transformers, and 125 PV systems. By using the single A matrix approach, the MV distribution grid can be modeled in a single A matrix that is a general approach. In the case of multiple A matrices approach, the MV distribution grid is separated into six subsystems (five radial feeders with one collector bus). Use case of steady-state operation case is considered to evaluate the accuracy and speed acceleration of the proposed simulation algorithms as compared to the baseline EMT simulation. All simulation were carried out in PSCAD by library components for the baseline case and by using Fortran script for the proposed algorithms. The EMT simulation was carried out for 0.25s, and the time between 0 and 0.05 is set for the simulation initialization. The simulation time step for all cases was $1\mu s$.

With the application of the proposed algorithms, the results have shown up to 22.4x and 326.4x in simulation time acceleration as listed in Table I. The comparison is with respect to the baseline EMT simulation model that was developed by using standard library components in PSCAD. The case of multiple A matrices shows higher speed-up due to smaller size of A matrices compared to the one in a single A matrix. However, the use of multiple A matrices may cause stability issue that is shown by relatively large high frequency oscillation in filter voltage during the initialization in Fig. 8-(a). The stability issues will arise only when the dynamics in the system interact with the time-step delay and/or the non-linearities present in the system. This is because there is the introduction of a single time step delay between the subsystems as discussed in Section III. In the simulation, 5nF of capacitors are added to each subsystem to reduce the initial high frequency oscillation. After 0.05s, the initialization is completed and, the oscillations are not observed thereafter.

TABLE I. Comparison of Measured Time for EMT Simulation

	Baseline	**Single A matrix**	**Multiple A matrices**
Time measured for 0.25s EMT simulation	58 hours	2.58 hours	0.18 hours
Speed-up	1x	22.4x	326.4x

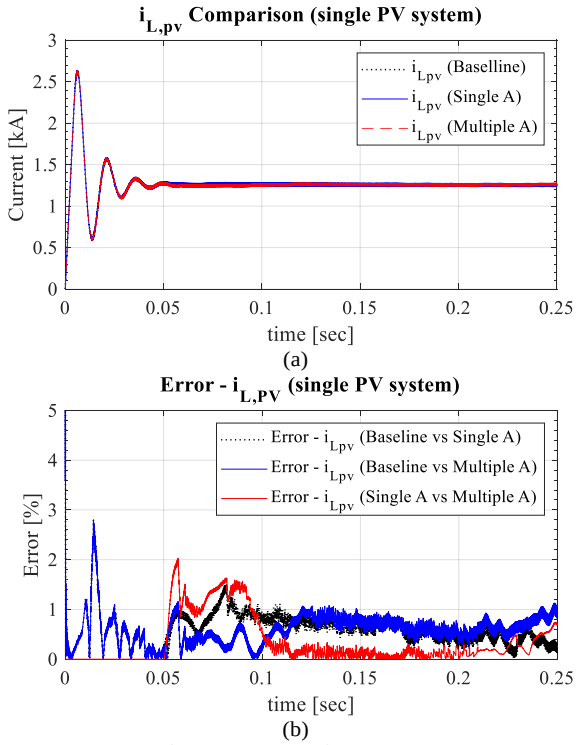

Fig. 6: Comparison of the simulation of MV distribution grid with large number of PV inverter modules based on the proposed simulation algorithms: (a) dc-dc boost converter inductor current ($i_{L,\mathrm{pv}}$) in one PV modules, (b) errors of the inductor current ($i_{L,\mathrm{pv}}$).

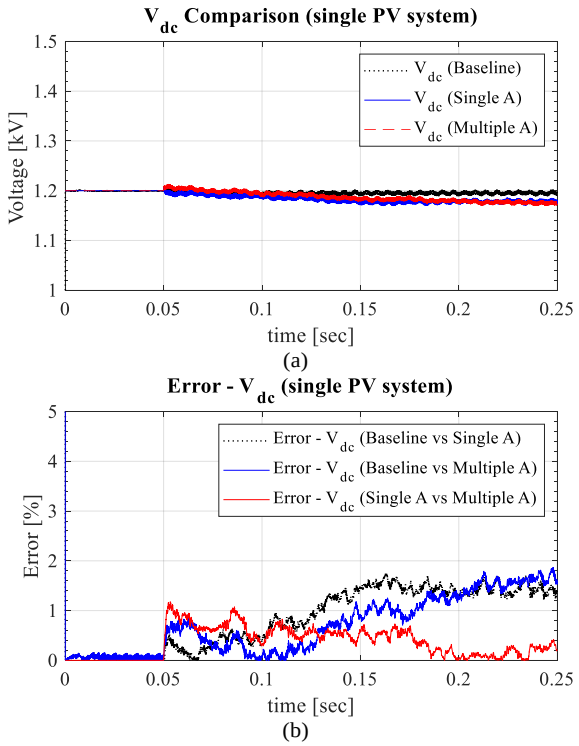

Fig. 7: Comparison of the simulation of MV distribution grid with large number of PV inverter modules based on the proposed simulation algorithms: (a) dc link voltage (v_{dc}), (b) error of the dc link voltage (v_{dc}).

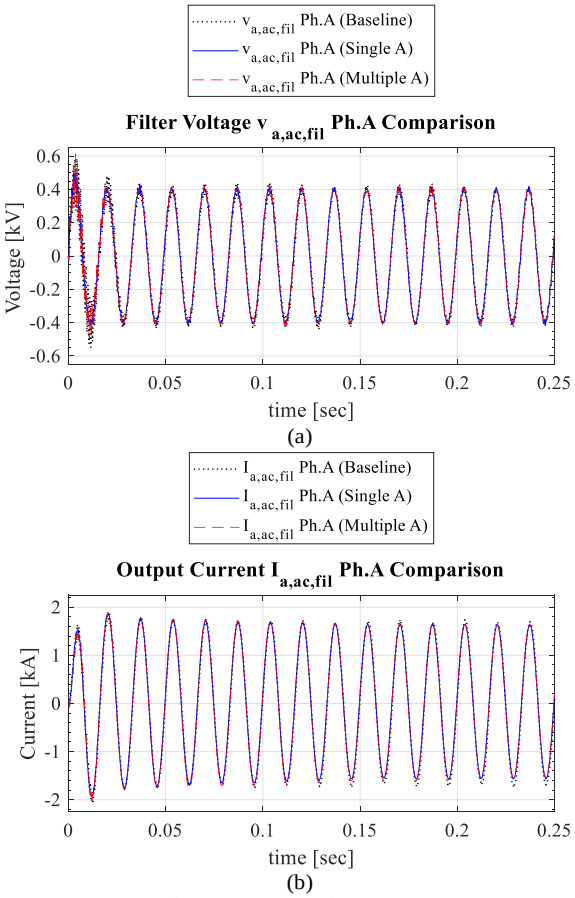

Fig. 8: Comparison of the simulation of MV distribution grid with large number of PV inverter modules based on the proposed simulation algorithms: (a) filter capacitor voltage ($v_{a,\mathrm{ac,fil}}$) phase A in one PV inverter modules, (b) dc-ac inverter output current ($i_{a,\mathrm{ac,fil}}$) phase A in one PV inverter modules.

Some of the states from the simulation results are illustrated to compare and evaluate the accuracy of the proposed algorithms. The inductor current of the dc-dc boost converter ($i_{L,\mathrm{pv}}$) in the PV inverter module and the associated errors between cases are compared between the cases of baseline, single A matrix, and multiple A matrices in Fig. 6. The results in Fig. 6-(a) present the similarity of the inductor currents between cases. The observed errors in Fig. 6-(b) indicate less than 2% during the simulation except for the initialization. The comparison of the dc link voltage (v_{dc}) in the PV inverter module and the associated errors between cases are shown in Fig. 7. The simulation results in Fig. 7 shows that all three cases of baseline, single A matrix, and multiple A matrices present similar trajectories of the states with less than 2% errors. The filter voltage ($v_{a,\mathrm{ac,fil}}$) and the inverter output current ($i_{a,\mathrm{ac,fil}}$) are illustrated in Fig. 8. The comparison of the voltages and currents in Fig. 8 shows the similarity between the simulation results. However, using multiple A matrices might cause numerical stability issue that is displayed in relatively high frequency oscillation in filter voltage during the initialization in Fig. 8-(a). This is because the multiple A matrices approach introduces a single time step delay between the subsystems as discussed in Section III. In the simulation, 5nF of capacitors are added to subsystem's terminals to reduce the initial high

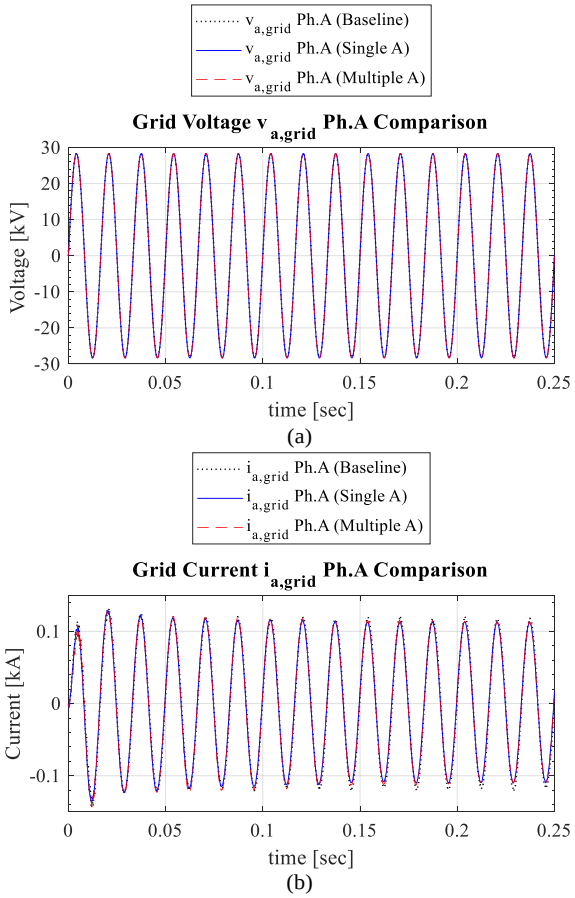

Fig. 9: Comparison of the simulation of MV distribution grid with large number of PV inverter modules based on the proposed simulation algorithms: (a) grid voltage ($v_{a,\text{grid}}$) phase A at the primary side of distribution transformer, (b) grid current ($i_{a,\text{grid}}$) phase A at the primary side of distribution transformer.

frequency oscillation. After 0.05s, the initialization is finished, the oscillation is not observed any longer. The grid voltage ($v_{a,\text{grid}}$) and the grid current ($i_{a,\text{grid}}$) at the primary side of one distribution transformer in the MV grid are illustrated in Fig. 9. The comparison of the voltages and currents in Fig. 9 shows the similarity between the simulation results.

V. Conclusion

In this paper, advanced numerical simulation approaches based on numerical stiffness-based hybrid discretization, DAEs clustering and aggregation, multi-order discretization, and matrix splitting algorithm have been developed to speed up the EMT simulation of a distribution grid with a large number of PV systems. The proposed algorithm has been applied to a 52-bus MV distribution grid consisting of 25 distribution transformers with 125 PV inverter modules. With the application of the proposed algorithms, the observed simulation speed has been increased by nearly up to 326x. The accuracy of the proposed EMT simulation algorithm has been evaluated by comparing states such as inductor current, dc-link voltage, inverter output current, filter voltage, grid current, and grid voltage at distribution transformer to the corresponding states of the baseline EMT model that is generally developed by using standard library components in PSCAD. The observed errors from the proposed algorithms-based simulation are less than 2%. This simulation algorithm can be applied to a large solar farm as well as a distribution grid with a great number of inverter-based distributed generation systems.

Acknowledgment

Authors would like to thank Kemal Celik for overseeing the project developments and providing guidance.

References

[1] N. Stephen and L. Angelina, “Annual Energy Outlook 2021.” [Online]. Available: https://www.eia.gov/outlooks/aeo/. [Accessed: 09-Mar-2021].

[2] NERC, “Improvements to Interconnection Requirements for BPS-Connected Inverter-Based Resources,” 2019.

[3] NERC, “Integrating Inverter- Based Resources into Low Short Circuit Strength Systems,” 2017.

[4] NERC, “1,200 MW Fault Induced Solar Photovoltaic Resource Interruption Disturbance Report,” 2017.

[5] NERC, “900 MW Fault Induced Solar Photovoltaic Resource Interruption Disturbance Report,” 2018.

[6] NERC and WECC, “April and May 2018 Fault Induced Solar Photovoltaic Resource Interruption Disturbances Report,” 2019.

[7] S. Debnath and M. Chinthavali, “Numerical-Stiffness-Based Simulation of Mixed Transmission Systems,” *IEEE Trans. Ind. Electron.*, vol. 65, no. 12, pp. 9215–9224, Dec. 2018.

[8] S. Debnath, P. R. V. Marthi, and J. Sun, “Advanced Modeling Fast Simulation Algorithms for Alternate Arm Converters,” in *2018 IEEE Electronic Power Grid (eGrid)*, 2018, vol. 4, pp. 1–6.

[9] S. Debnath and P. R. V. Marthi, “Advanced Modeling & Fast Simulation Algorithms for Cascaded Two-Level Converters,” in *2018 IEEE Electronic Power Grid (eGrid)*, 2018, vol. 4, pp. 1–6.

[10] F. Dorfler and F. Bullo, “Kron Reduction of Graphs With Applications to Electrical Networks,” *IEEE Trans. Circuits Syst. I Regul. Pap.*, vol. 60, no. 1, pp. 150–163, Jan. 2013.

[11] S. Y. Caliskan and P. Tabuada, “Towards Kron reduction of generalized electrical networks,” *Automatica*, vol. 50, no. 10, pp. 2586–2590, Oct. 2014.

[12] K. Strunz and E. Carlson, “Nested fast and simultaneous solution for time domain simulation of integrative power electric and electronic systems,” in *2009 IEEE Power & Energy Society General Meeting*, 2009, vol. 22, no. 1, pp. 1–1.

[13] A. Floriduz, M. Tucci, S. Riverso, and G. Ferrari-Trecate, “Approximate Kron Reduction Methods for Electrical Networks With Applications to Plug-and-Play Control of AC Islanded Microgrids,” *IEEE Trans. Control Syst. Technol.*, vol. 27, no. 6, pp. 2403–2416, Nov. 2019.

.